




Multi-objective optimization on turning of additively manufactured Inconel 625 alloy using grey relational analysis

Muthukumaran Kathavarayan¹, Arul Kulandaivel², Visagan Arjunan¹

¹Anna University, Madras Institute of Technology, Department of Production Technology. Chromepet, Chennai, Tamil Nadu, India.

²Agni College of Technology, Department of Mechanical Engineering. Thalambur, Chennai, Tamil Nadu, India.

e-mail: mkkumaran561@gmail.com, arulroll7@gmail.com, visaganarjunan69@gmail.com

ABSTRACT

The unique properties of Inconel 625 make it desirable for engineering applications. It is expensive and complex to machine Inconel 625 due to its unique properties. In light of the widespread use of turned components in crucial aircraft engines, the turning method was chosen to evaluate the impact of turning parameters on cutting forces, surface roughness, material removal rate and temperature. In this study, the Taguchi optimization approach is applied to optimize cutting parameters with laser textured tungsten carbide with HBN nano particle filled cutting tools during high-speed turning of Inconel 625. The cutting parameters include the depth of cut, feed rate, and speed at which the work piece is turned. ANOVA was used to identify the most influencing process parameters on the turning operation. The cutting speed of 14 m/min, Feed rate of 0.3 mm/rev and depth of cut of 0.33 mm gave a better cutting force of 239 N and material removal rate of 3.22 mm³/min and also a reduced surface roughness to 2.834 μm , and temperature of 61°C. From ANOVA, feed rate 77.38% was identified the most influencing process parameter on the turning operation followed by cutting speed 8.65% and depth of cut 0.41%.

Keywords: Turning; Inconel 625 alloy; Selective laser melted; Taguchi GRA; ANOVA.

1. INTRODUCTION

Super alloys based on nickel have been widely used in the nuclear, chemical, petrochemical, and aerospace sectors because of their superior thermo-mechanical characteristics. However, because of their difficult to cut nature and the extremely high cutting pressures that result in work hardening, surface ripping, and distortion in the final machined components, they offer major problems to the manufacturing industry [1]. Engine parts, heat exchangers, pressure valves, and other items have been made using Inconel 625, a super alloy based on nickel that has been solution strengthened. Selective laser melting (SLM), a type of laser-based additive manufacturing, has been investigated over the past ten years to produce functioning metal objects with complex internal structures and almost complete densities straight from CAD models [2]. In order to minimize tool wear and surface roughness machining parameters for turning Inconel 625 in a refrigerated air cooling environment. The optimal machining parameters for Inconel 625 are as follows: cutting velocity of 50 m/min, feed rate of 0.11 mm/rev, depth of cut of 0.2 mm, and surface roughness of 0.5841 μm at desirability level 0.779. Tool wear is anticipated to be 163.124 μm . Confirmation testing showed that the error (%) between the measured and anticipated values for surface roughness and tool wear is within allowable bounds. The findings indicate that when compared to dry machining settings, cold air jet (CAJ) turning yields 11.76% greater tool life and 19.67% improved surface quality. Moreover, compared to dry machining, tool life improvement in CAJ turning can reach 15% at a deeper cut depth of 0.4 mm. A high-speed turning operation on Inconel 625 was performed by WAGHMODE and DABADE [3] in order to investigate the effects of surface roughness and cutting forces on input parameters. In turning experiments, Taguchi's orthogonal array L9 was used. Analyzing the outcomes requires the use of the analysis of variance (ANOVA) technique. In this analysis, the parameters are represented by their % contribution. It has been observed that cutting forces tend to increase as cut depth and feed rate increase, but cutting speeds tend to decrease. AKGÜN and DEMİR [4] developed a mathematical model for surface roughness (Ra) in the turning of Inconel 625 super alloy with cryogenically treated tungsten carbide inserts. The impact of cryogenic treatment on tungsten carbide tool microstructure and hardness was also examined for the as-received inserts and deep cryogenic treatment at 196°C for 12, 24, and 36 hours. As part of an orthogonal

array L16, turning tests were conducted at various levels of cutting tool, feed rate, and cutting speed. In order to evaluate the cutting settings, we measured the roughness of the surface (R_a). An analysis of variance was used to determine the proportion of each cutting component. The Minimum Quantity Lubrication Setup might significantly reduce the cutting force, temperature, roughness of the surface, and wear on the tool. The lubricant, especially when sprayed at the greatest dosage, produced smoother surfaces with fewer scratches and less plastic deformation. A stronger material resistance to deformation was produced by lower cutting temperatures in the cutting zone, which was credited with this improvement [5]. Hexagonal Boron Nitride (HBN) has not been employed as a solid lubricant in any of the earlier experiments on tungsten carbide tools to improve machining efficiency. Cutting force, roughness, material removal rate, and temperature have never been evaluated prior to this study. The surface integrity of Inconel 625 made additively using HBN as a filler in carbide-coated tools was not assessed [6]. It is evident from the above considerations that additive manufacturing (AM) technology, namely selective laser melting (SLM), has great potential for fabricating components made from Inconel 625 that are complex in shape. While additive manufacturing allows for greater design freedom [7]. Numerous scholars have thoroughly examined the mechanical characteristics of Inconel 625, which is manufactured using the SLM method [8]. Inconel 625 mechanical and microstructural characteristics are further detailed in other reports [9]. The overview of the literature demonstrates how little research was done on the surface and subsurface characteristics of Inconel 625 as a result of post processing procedures.

RIVERA *et al.* [10] analyzed the microstructural behavior and mechanical properties of IN625 produced by AFS process. The grains as small as $0.27\ \mu\text{m}$ were seen at the layer interfaces with the help of Electron Back Scatter Diffraction (EBSD). In other parts of the formed layers, the average grain size was about $1\ \mu\text{m}$. It was looked at how the yield and final tensile strengths of fine-grained materials changed with increasing strain rates, both at a quasi-static ($0.001/\text{s}$) rate and a high rate ($1500/\text{s}$). The HS results had an engineering strength that was about 200 MPa higher than the QS results. At both strain rates, the fracture surfaces aligned with the highest shear plane and featured micro voids. Heat-treated SLMed IN 625 samples were microstructurally evaluated by LI *et al.* [11] using optical metallography, SEM, EBSD, TEM, X-ray diffraction, and microindentation. As-SLM samples exhibited fine dendritic microstructures with a high correlation to layer accumulation. After cooling quickly, they developed epitaxially. The γ matrix is microhard and features many dislocations. It also has several high-Z-contrast precipitates. High-temperature annealing causes random grain development, dislocation, destruction, and twinning. Less residual stress is seen after SLM when the lattice parameters are smaller and there is common big grain boundary misorientation in the γ matrix.

Erliang LIU *et al.* [12] performed optimization of turning parameters on Inconel 625 superalloy using PVD-TiAlN coated carbide tools. The depth of cut was 0.5 mm, cutting speed was ranged from 25–175 mm/min, and feed was ranged from 0.02–0.3 mm/r. The responses selected for optimization are surface roughness and flank wear. Results showed that as the cutting speed v_c and feed rate f increased further, the tool began to peel, tip, or even fracture. The optimum parameter for obtaining a better surface finish and flank wear is by selecting the cutting speed at 60m/min, feed at 0.1 mm/r and depth of cut at 0.5 mm. VENKATESAN and RAMANUJAM [13] examined how cutting parameters impact shaping Inconel 625, a Ni-Cr alloy with PVD AlTiN-coated carbide inserts. The experimental arrangement was designed using Taguchi L9 orthogonal array. The investigation was carried out by considering three levels of cutting speed, feed rate, and depth of cut, and the output responses were cutting force and surface roughness. The most influential parameter on output responses was found using ANOVA. The cutting speed was the most influencing factor, depth of cut had the least effect, followed by feed rate and surface roughness. The cutting force was most affected by feed rate and depth of cut, whereas cutting speed had little effect. The regression model built for the study improved surface roughness and cutting force and predicted a near value to the experimental value.

RAJGURU and VASUDEVAN [14] examined the impact of process parameters on the micro-hardness of the machined surface and subsurface of Inconel 625 during dry milling with a TiAlSiN-coated tool. The study found that the process parameters, particularly when using a TiAlSiN-coated tool, had a low influence on the micro-hardness gradient in the top layer of the machined surface. This indicates that the coating and dry machining conditions stabilize the hardness near the surface despite varying parameters. Balancing the mechanical and thermal effects through parameter adjustment can significantly enhance machining performance and surface quality. KREBS and POLLI [15] investigated the turning of Inconel 625, clad on AISI 4130 steel, using different tool materials under various machining conditions. The SiAlON inserts proved feasible for rough turning Inconel 625 clad on steel. A low cutting speed of 140 m/min led to significant flank and notch wear on the SiAlON inserts, along with burr formation and intensive adhesion. The optimum combination for getting a better response were at a cutting speed of 160 m/min and a feed rate of 0.25 mm/rev. By decreasing the intensity of wear mechanisms and enhancing cutting efficiency, these parameters reduced flank and notch wear.

RAKESH and CHAKRADHAR [16] improved Inconel 625's machining performance using cryogenic machining, which addresses the material's strong strength at high temperatures. Using Taguchi's L9 orthogonal array, cutting speed, feed rate, and depth of cut were set at three levels, and surface roughness, flank wear, and cutting force were assessed. The ANOVA showed that feed rate (89.84%) affects output responses the most, followed by depth of cut (3.08) and cutting speed (2.29%). By minimizing cutting forces, tool wear, and surface roughness, 60 m/min cutting speed, 0.05 mm/rev feed rate, and 0.2 mm depth of cut enhanced machining performance. SEM has helped explain wear and chip formation, proving cryogenic machining works in some cases. SINGH *et al.* [17] investigated the application of nano-fluid minimal quantity lubrication (NMQL) as a potential substitute for conventional cutting fluids in the machining process of Inconel 625, a material known for its limited machinability. The implementation of NMQL led to reduced tool wear in comparison to dry machining and showed comparable effectiveness to flood machining. The utilization of NMQL resulted in a surface finish that was similar to that obtained by flood cooling, showcasing its efficiency in improving the quality of machining processes. NMQL, or nano-fluid minimum quantity lubrication, is a more environmentally friendly alternative to traditional cutting fluids. It works well with the goals of eco-friendly and cost-effective machining methods.

OZBEK *et al.* [18] studied the influence of cutting parameters, including cutting speed, feed rate, and cutting tool coatings, on various machining responses such as cutting temperature, vibration, surface roughness, and noise. The Taguchi L18 orthogonal array was used for carrying out the experiments and the parameters were varied at three different levels. Results indicated that an increase in feed rate generally results in increased surface roughness due to the higher feed rate, which leaves more pronounced tool marks on the machined surface. At higher feed rates increased cutting force, surface roughness, and vibration levels due to the higher material removal rate were observed. The PVD coatings often result in lower surface roughness and cutting forces compared to CVD coatings due to their higher hardness and lower friction coefficients. The results from ANOVA showed that feed rate had the maximum influence on surface roughness and noise while on the other hand cutting tool type had the maximum influence on vibration. AKGUN and KARA [19] investigated the effects of cutting parameters on cutting force (F_c) and surface roughness (R_a) using uncoated and PVD-TiB₂ coated cutting inserts. Taguchi method was implemented for experimental design and ANOVA was used to determine the significance of various cutting parameters on machining performance. The feed rate has a significant impact on cutting force, with increased feed rates leading to higher cutting forces due to the greater amount of material being removed per unit time. The performance of coated vs. uncoated tools can vary depending on the material being machined, cutting conditions, and the type of coating used. The developed mathematical models for cutting force (F_c) and surface roughness (R_a) present reliable results with coefficients of determination (R^2) of 96.04% and 92.15%, respectively.

BATISTA *et al.* [20] explored the effects of preheating, interpass temperature, and stress relief heat treatment on the microstructure, microhardness, and chemical composition gradient of welds made with AWS E NiCrMo3 alloy on quenched and tempered AISI 8630M and AISI 4130 steels. The excessive temperatures during the process led undesirable metallurgical transformations, such as grain coarsening or increased brittleness in the heat-affected zone (HAZ). The reduction in microhardness due to stress relief is typically attributed to the relaxation of lattice strains and the reduction of dislocation density. The PTA-P welding generally results in finer microstructures, less dilution, and fewer partially diluted zones (PDZs) compared to MIG welding, which often produces welds with varying morphologies and higher degrees of dilution.

The experimental work presented in this article focuses on how the input parameters such as cutting speed, feed and depth of cut affects the cutting force, surface roughness, material removal rate and temperature during the turning of Inconel 625 specimens made utilizing the SLM technique. The carbide inserts were subjected to laser texturing and the spaces were filled with HBN nano particles. The HBN nano particles filled inside the carbide inserts acts as solid lubricant thereby enhancing the dissipation of heat at the contact region between the tool and workpiece. Taguchi L9 orthogonal array was used to identify the optimal combination of input process parameter for obtaining better responses. The ANOVA was used to identify the most influencing process parameter on turning of Inconel 625 using HBN carbide inserts.

2. MATERIALS AND METHODS

Inconel 625, a material created using additive manufacturing, served as the work piece material for the study. Selective Laser Melting (SLM), a 3D printing technique, was used to create it. A relatively recent development in 3D printing technology is selective laser melting (SLM). The SLM method builds 3D objects using a laser beam, similar to the UV laser method used for SLA. The SLM technique's basic idea is to apply a very thin coating of metallic powders to a construction platform. These powders are then completely fused or melted, and one or more laser beams are employed to provide thermal energy. In the SLM process, powders with particle sizes between 20 and 50 microns and layers between 20 and 100 microns are often used. Several biodegradable

metals have been found using the SLM process, including Zn, Mg, Cu, Cr, and Co-Cr, and stainless steel, Al, and Ti alloys [21]. In the printing process, different metallic particles are melted and fused together by the laser beam. In a thin layer of material, the laser beam welds or connects the particles selectively.

3. RESULTS AND DISCUSSION

3.1. Taguchi grey relational analysis

To create the necessary tables, such as the L9 orthogonal array reported in Table 1, the Minitab 17 tool was utilized. The traditional approaches to quality control mostly depended on examining items as they came off the assembly line and rejecting those that did not fit within a predetermined acceptable range. But Taguchi was also keen to point out that quality has to be built into a product from the beginning; examination alone cannot make a product better. A standardized process for figuring out the ideal mix of inputs to create a good or service is the Taguchi technique. The design of experiments (DOE) is used to achieve this [22]. The process parameters for turning Inconel 625 have been determined and are listed in Table 1. Cutting speed, feed rate, and depth of cut are the three regulated elements that may be adjusted for three levels each to efficiently cover the whole range that the machine tool can access. The design and process engineer's toolkit includes DOE, which is a crucial instrument. It offers a way to statistically pinpoint the precise components that work well together to create a high-quality good or service. Taguchi takes a four-pronged approach to design: idea design, tolerance design, resilient design, and parameter design. The Taguchi technique mainly concentrates on parameter design out of these four design factors [23]. The experimental layout and the obtained output responses are shown in Table 2. The machined samples are shown in Figure 1(d).

In optimization processes, the goal is often to maximize the S/N ratio. By improving the S/N ratio, engineers aim to minimize variability or deviation from desired specifications, thereby enhancing product quality or process performance. The larger the better criteria were used for Cutting force and Material removal rate using Equation (1) and smaller the better were used for surface roughness and temperature using Equation (2). The S/N ratio and Normalised S/N ratio for the output responses are shown in Table 3.

Table 1: Process parameters and their levels.

INPUT FACTORS		LEVELS		
		LEVEL 1	LEVEL 2	LEVEL 3
Cutting Speed (m/min)	A	14	17	20
Feed Rate (mm/rev)	B	0.2	0.26	0.33
Depth of Cut (mm)	C	0.1	0.2	0.3

Table 2: Process parameter combinations and output responses.

TRAIL NO.	PARAMETER LEVEL			RESPONSES			
	CUTTING SPEED	FEED RATE	DEPTH OF CUT	CUTTING FORCE	SURFACE ROUGHNESS	MATERIAL REMOVAL RATE	TEMPERATURE
Symbol	A	B	C	CF	RA	MRR	T
Units	(m/min)	(mm/rev)	(mm)	(N)	(μm)	(mm^3/min)	($^{\circ}\text{C}$)
1	14	0.2	0.1	186	2.584	2.143	68
2	14	0.26	0.2	216	2.452	2.37	65
3	14	0.33	0.3	235	2.834	3.22	66
4	17	0.2	0.2	128	2.475	2.062	69
5	17	0.26	0.3	353	1.136	2.271	67
6	17	0.33	0.1	157	1.063	3.79	75
7	20	0.2	0.3	226	1.071	2.534	78
8	20	0.26	0.1	294	1.444	2.362	79
9	20	0.33	0.2	226	1.964	2.354	92

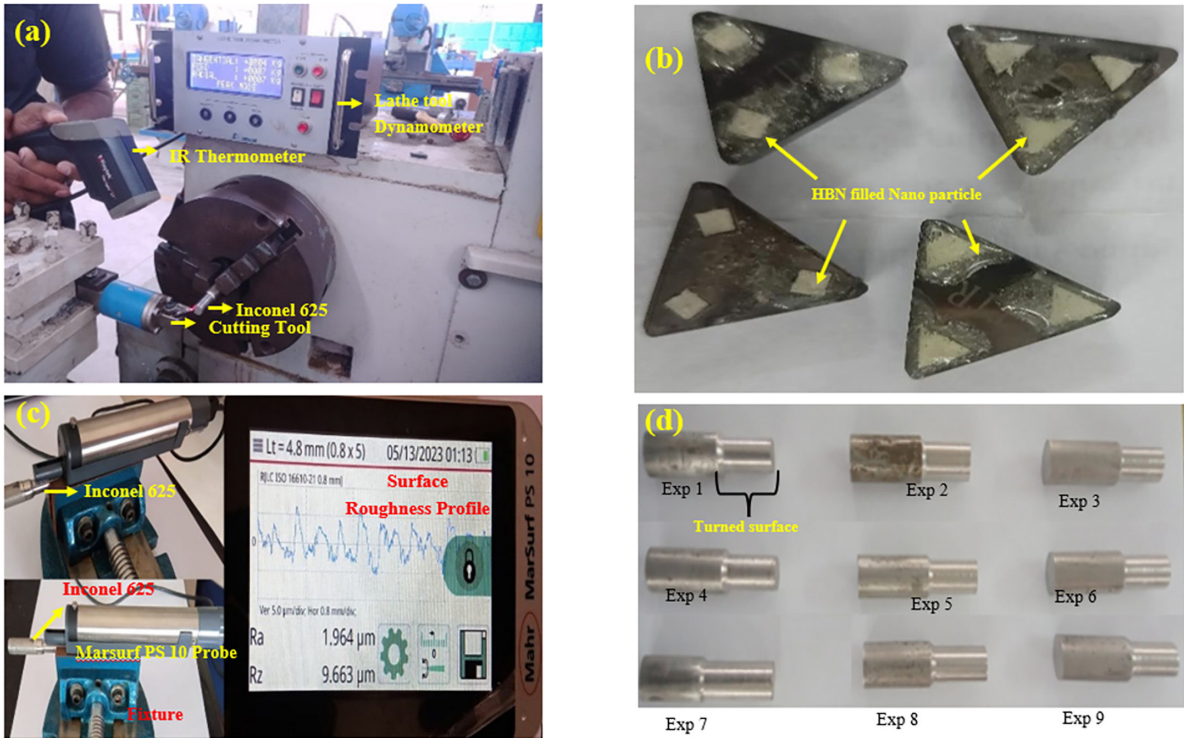


Figure 1: (a) Experimental setup (b) HBN filled WC inserts (c) MarSurf PS 10 Surface measurement device (d) Inconel 625 machined components.

Table 3: S/N ratio and normalised S/N ratio of output responses.

TRAIL NO.	S/N RATIO				N S/N RATIO			
	CF	RA	MRR	T	CF	RA	MRR	T
1	45.3903	-8.2459	6.6204	-36.6502	0.3684	0.9058	0.0633	0.1299
2	46.6891	-7.7904	7.4950	-36.2583	0.5158	0.8523	0.2287	0.0000
3	47.4214	-9.0480	10.1571	-36.3909	0.5989	1.0000	0.7322	0.0439
4	42.1442	-7.8715	6.2858	-36.7770	0.0000	0.8619	0.0000	0.1719
5	50.9555	-1.1076	7.1243	-36.5215	1.0000	0.0677	0.1586	0.0872
6	43.9180	-0.5307	11.5728	-37.5012	0.2013	0.0000	1.0000	0.4119
7	47.0822	-0.5958	8.0761	-37.8419	0.5604	0.0076	0.3386	0.5248
8	49.3669	-3.1913	7.4656	-37.9525	0.8197	0.3124	0.2232	0.5615
9	47.0822	-5.8628	7.4361	-39.2758	0.5604	0.6260	0.2176	1.0000

For ‘smaller the better’, S/N ratio = $-10\log_{10} \left(\frac{1}{n} \sum_{i=1}^n (Y_{ij2}) \right)$ (1)

For ‘larger the better’, S/N ratio = $-10\log_{10} \left(\frac{1}{n} \sum_{i=1}^n (1/Y_{ij2}) \right)$ (2)

For ‘smaller the better’, N S/N ratio, $Z_{ij} = \frac{(MaxY_{ij} - Y_{ij})}{(MaxY_{ij} - MinY_{ij})}$ (3)

For ‘larger the better’, N S/N ratio, $Z_{ij} = \frac{(Y_{ij} - MinY_{ij})}{(MaxY_{ij} - MinY_{ij})}$ (4)

Table 4: Grey relational coefficient and grey relational grade.

TRAIL NO.	GRC				GRG	RANK
	CF	RA	MRR	T		
1	0.4419	0.8415	0.3480	0.3649	0.4991	7
2	0.5080	0.7720	0.3933	0.3333	0.5017	6
3	0.5549	1.0000	0.6512	0.3434	0.6374	1
4	0.3333	0.7835	0.3333	0.3765	0.4567	8
5	1.0000	0.3491	0.3727	0.3539	0.5189	5
6	0.3850	0.3333	1.0000	0.4595	0.5445	3
7	0.5321	0.3350	0.4305	0.5127	0.4526	9
8	0.7350	0.4210	0.4500	0.5328	0.5347	4
9	0.5321	0.5721	0.3899	1.0000	0.6235	2

Table 5: Optimum table for weighted GRG.

INPUT PARAMETER		AVERAGE WEIGHTED GRG				RANK
		LEVEL 1	LEVEL 2	LEVEL 3	RANGE	
Cutting Speed (m/min)	A	0.5460 [#]	0.5067	0.5369	0.04	2
Feed Rate (mm/rev)	B	0.4695	0.5184	0.6018 [#]	0.13	1
Depth of Cut (mm)	C	0.5261	0.5273	0.5363 [#]	0.01	3

Total Grey Relational Grade = 0.5299, # Optimum parameter level

The Grey Relational Coefficient (GRC) and Grey Relational Grade (GRG) are calculated using Equation (5) and Equation (6) respectively and shown in Table 4.

For GRC,

$$\xi_{ij} = \frac{\Delta_{Min} + \lambda \Delta_{Max}}{Y_{ij} + \lambda \Delta_{Max}} \tag{5}$$

where, λ - distinguishing coefficient, ($0 \leq \lambda \leq 1$). Here the distinguishing coefficient is taken as 0.5. The highest value of GRG is ranked as 1.

$$G_i = \frac{1}{m} \sum_{j=1}^m \xi_{ij} \tag{6}$$

The single GRG now optimizes the multi-objective optimization [24] and high GRG indicates that the relationship between the ideal sequence and the present sequence is better. A higher GRG means that the obtained responses are closer to the actual output of the process. Accordingly, as shown in Table 5 the optimal sequence of input process parameters was chosen as follows: Cutting Speed (A1 = 14 m/min), Feed Rate (B3 = 0.3 mm/rev) and Depth of Cut (C3 = 0.33 mm).

4. ANOVA STUDY

The ANOVA method assigns proportions to multiple inputs based on the variation of the Response variable. The highest contributing factor for the responses under consideration is determined using ANOVA [25] as shown in Figure 2. From Table 6 it can be seen that Feed rate has the maximum contribution of 77.38% followed by cutting speed having 8.65% and a minimum contribution by Depth of cut having 0.41%.

5. VALIDATION EXPERIMENT

Finally, in order to verify the Taguchi Grey Relational Analysis approach that was implemented for multi-response optimization, a validation experiment was with the most optimal process parameter settings to achieve the most desirable results as shown in Table 7. The validation experiment was conducted by setting the cutting

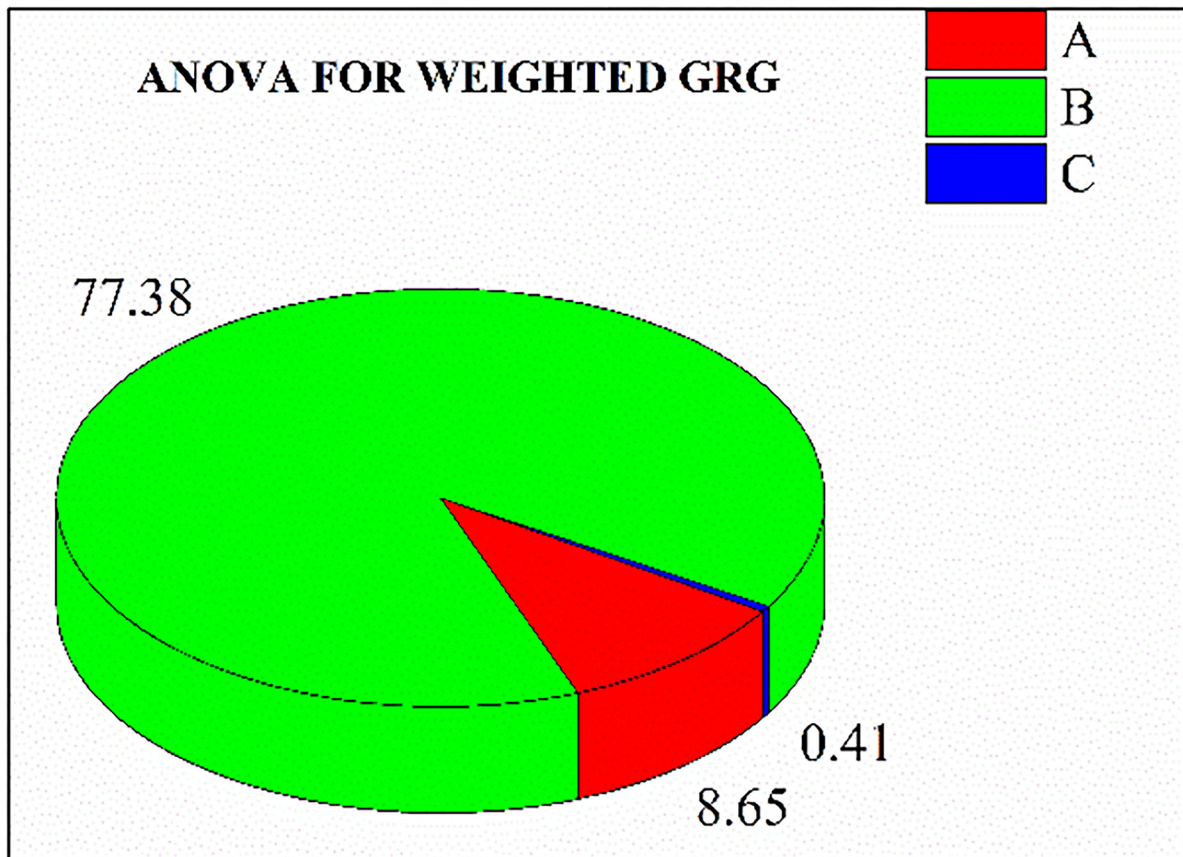


Figure 2: ANOVA for weighted GRG.

Table 6: Results of ANOVA for weighted GRG.

INPUT PARAMETER	SOURCE	DF	SUM OF SQUARE	MEAN SQUARE	CONTRIBUTION
Cutting Speed (m/min)	A	2	0.002875	0.001437	8.65%
Feed Rate (mm/rev)	B	2	0.025730	0.012865	77.38%
Depth of Cut (mm)	C	2	0.000135	0.000067	0.41%
Error		2	0.004512	0.002256	13.57%
Total		8			100.00%

Table 7: Validation experiment.

RESPONSES	INITIAL PARAMETER LEVELS A1B3C3	OPTIMAL PARAMETERS LEVELS A1B3C3	DIFFERENCE	ERROR (%)
Cutting Force	235	239	0.016736	1.67364
Surface Roughness	2.834	2.217	-0.278304	-27.8304
Material Removal Rate	3.22	3.55	0.092958	9.295775
Temperature	66	61	-0.081967	-8.19672

speed of 14 m/min, feed rate of 0.33 mm/rev, depth of cut at 0.3mm, i.e A1B3C3. It can be observed that the cutting force and material removal has been increased from 235 N to 239 N and 3.22 mm³/min to 3.55 mm³/min respectively. Similarly, the surface roughness and temperature has been significantly reduced from 2.834 μm to 2.217 μm and 66°C to 61°C respectively.

6. EFFECT OF PROCESS PARAMETERS ON OUTPUT RESPONSES

6.1. Cutting force

Cutting force is the material’s ability to withstand the cutting tool’s penetration. A lathe instrument called a dynamometer is used to measure cutting force. For the Inconel 625 to spin smoothly, the cutting forces generated should be smaller [26]. Figure 3(a), shows the primary impact plot for the S/N Ratio of Cutting force. The response table for the S/N ratio for cutting force is displayed in Table 8. The ideal process parameters are for getting the optimal cutting force is at a cutting speed of 20 m/min, feed rate of 0.26 mm/rev, and a depth of cut of 0.3 mm i.e (A3B2C3). From Figure 3(a) it can be clearly seen that among the three-input parameter Feed rate had the highest influence on cutting force.

6.2. Surface roughness

The total number of evenly spaced abnormalities on the surface is expressed as the surface roughness. Surface roughness significantly affects the product’s performance and longevity. It facilitates the creation of dependable goods and uniform procedures. The MarSurf PS10 as shown in Figure 3(a) was used to measure the surface roughness of the machined components. For optimal performance, the resultant roughness should typically be lower. Table 9 shows the roughness S/N ratio for surface roughness. The ideal parameters for obtaining a better surface roughness are a cutting speed of 17 m/min, feed rate 0.26 mm/rev, and depth of cut 0.3 mm i.e (A2B2C3). The cutting speed has a greater effect on surface roughness, therefore cutting speed must be lowered to minimize surface roughness as shown in Figure 3(b).

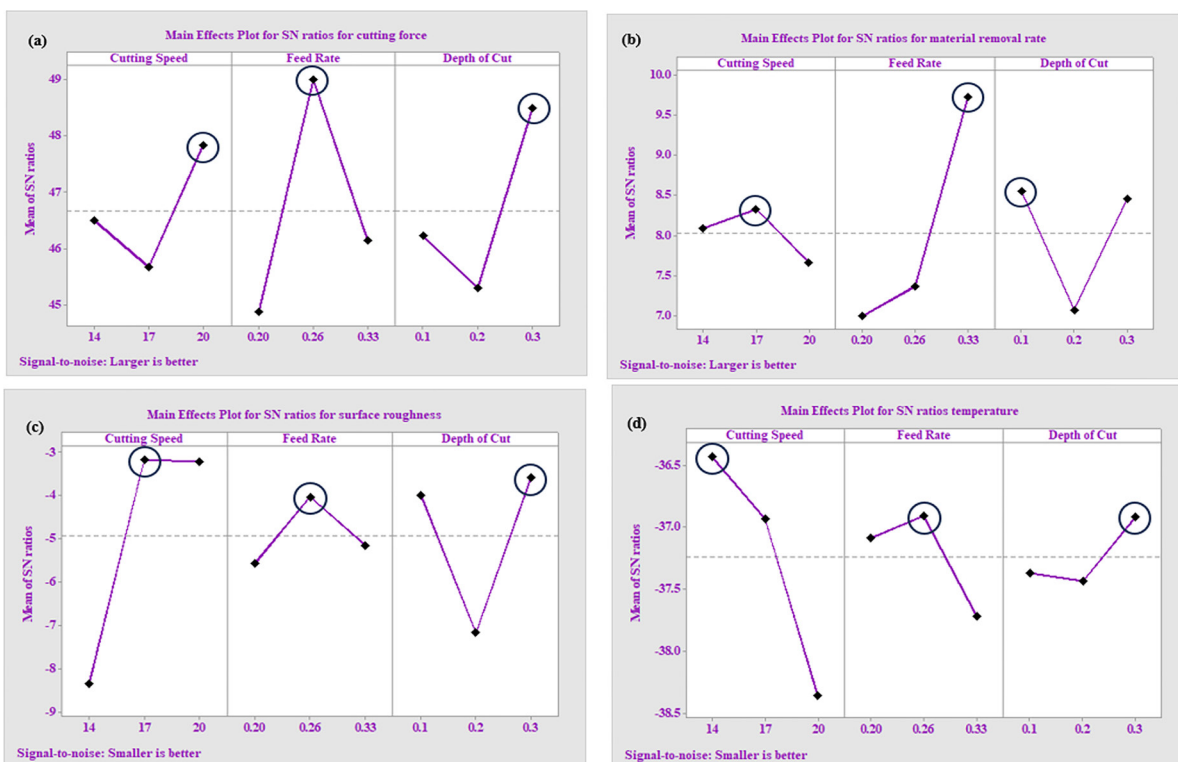


Figure 3: (a-d) Main effect plots for output responses.

Table 8: Response table for S/N ratio for cutting force.

LEVEL	CUTTING SPEED	FEED RATE	DEPTH OF CUT
1	212.3	180	212.3
2	212.7	287.7	190.0
3	248.7	206.0	271.3
Delta	36.3	107.7	81.3
Rank	3	1	2

Table 9: Response table for S/N ratio for surface roughness.

LEVEL	CUTTING SPEED	FEED RATE	DEPTH OF CUT
1	2.623	2.043	1.697
2	1.558	1.677	2.297
3	1.493	1.954	1.680
Delta	1.130	0.366	0.617
Rank	1	3	2

Table 10: Response table for S/N ratio for material removal rate.

LEVEL	CUTTING SPEED	FEED RATE	DEPTH OF CUT
1	2.578	2.246	2.765
2	2.708	2.334	2.262
3	2.417	3.121	2.675
Delta	0.291	0.875	0.503
Rank	3	1	2

Table 11: Response table for S/N ratios for temperature.

LEVEL	CUTTING SPEED	FEED RATE	DEPTH OF CUT
1	66.33	71.67	74.00
2	70.33	70.33	75.33
3	83.00	77.67	70.33
Delta	16.67	7.33	5.00
Rank	1	2	3

6.3. Material removal rate

The material removal rate is determined by how much material is removed per unit of time from the work piece. In order to calculate the material removal rate, the amount of material removed or the change in weight can be used. The MRR is calculated using the Equation (7).

$$\text{Material removal Rate} = \frac{\text{Initial Weight} - \text{Final Weight}}{\text{Machining Time}} \quad (7)$$

The response table for the S/N Ratio for Material Removal Rate is displayed in Table 10. For optimal performance, a cutting speed of 17 m/min, a feed rate of 0.33 mm/rev, and a cut depth of 0.1 mm i.e (A2B2C1) are selected as the process parameters. Feed rate has the highest influence on getting a better MRR as shown in Figure 3(c).

6.4. Temperature

It is important to maintain a low temperature throughout the turning operation since a high temperature might result in excessive tool wear and increased surface roughness. Because HBN has strong thermal characteristics and helps to reduce the temperature created during turning, tungsten carbide inserts packed with HBN are used to turn Inconel 625, therefore avoiding tool wear. Here, an infrared thermometer is used to measure the temperature. The response table for S/N Ratios for Temperature is displayed in Table 11. In order to achieve optimal temperature, a cutting force of 14 m/min, feed rate of 0.26 mm/rev, and depth of cut of 0.3 mm i.e (A1B2C3) are selected as the ideal process parameters. The cutting speed has the most significant influence on the temperature of the process as shown in Figure 3(d).

6.5. SEM and EDS analysis

A surface with comparatively fewer imperfections was found by SEM analysis, suggesting a higher quality material. Granular thick cracks, torn edges, evidence of ductile failure in the vicinity of inclusions, and the

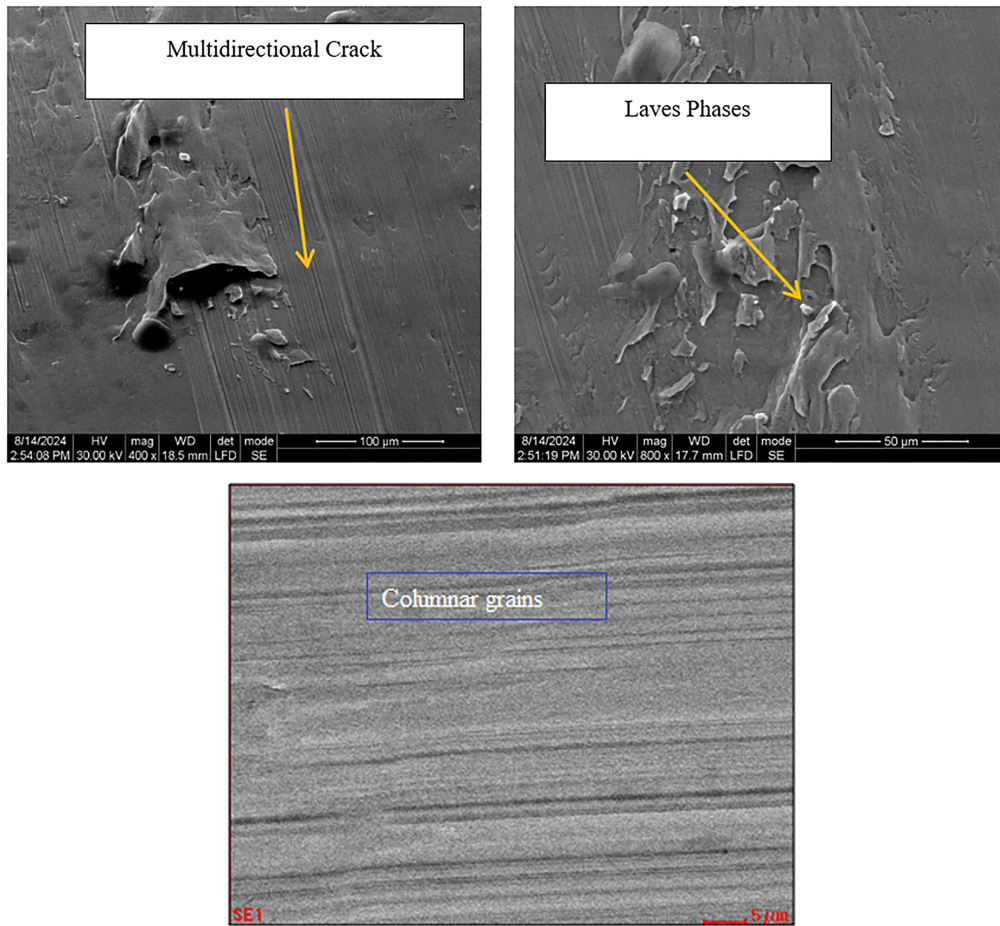


Figure 4: SEM image of Inconel 625 alloy.

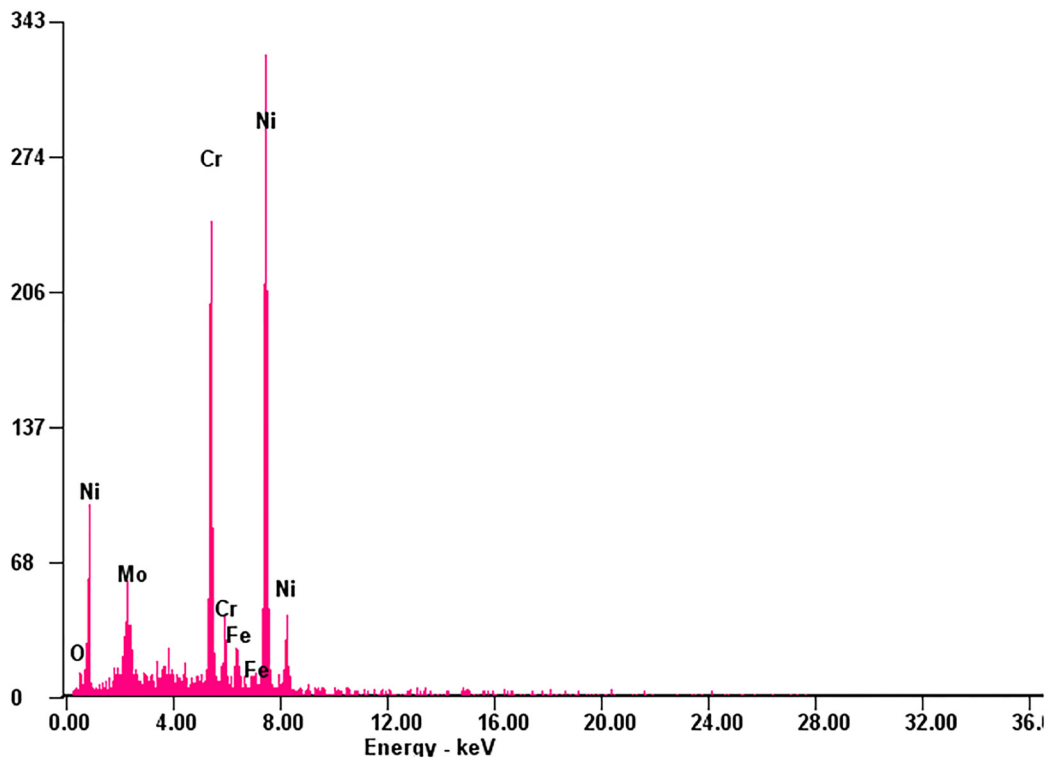


Figure 5: EDS report for Inconel 625 alloy.

existence of micro voids were a few prominent surface characteristics that were noticed as shown in Figure 4. The granular thick cracks imply the possibility of inclusion-related localized fracture brought on by large stress concentrations. Broken edges show how cracks spread during the failure process, whereas ductile failure close to inclusions indicates localized plastic deformation. Micro-voids enhance the significance of material failure mechanisms, including void coalescence. SEM investigation, on the other hand, revealed unique characteristics on its cracked surface. These characteristics were striations and deep, granular fractures. The existence of localized fracture or areas of concentrated stress is suggested by the granular thick fractures as shown in Figure 4. Striations can be caused by fatigue or dynamic loading conditions. They are a sign of cyclic crack growth or repetitive loading cycles. In addition, the elemental makeup of the samples was ascertained using EDS analysis. Based on the EDS examination, all of Inconel 625's elements were found to be within a good range in the sample as shown in Figure 5. These components verify the material's makeup and compatibility with the anticipated Inconel 625 alloy. As a result, about 28.54% of the Inconel 625 powder was transformed into the NbC and Laves phases under microwave irradiation.

7. FUTURE SCOPE OF STUDY

The turning process of Inconel 625 alloy using the HBN filled carbide inserts can be performed by varying the parameters and also by increasing the number of experiments. The material of the workpiece may also be changed for the necessary applications. The shape of the HBN nano particle present on the surface of the carbide inserts can be reconstructed for some other shape in order to study the change in output responses. The solid lubricant may also be replaced with a nano Minimum Quantity Lubrication (MQL) method and the responses maybe analyzed.

8. CONCLUSION

The current work firmly proves that the Taguchi Grey Relational Analysis is an effective optimization tool for turning of selective laser melted Inconel 625 alloy using HBN filled carbide inserts. The following were the results obtained from the current work:

- i) The ideal process parameters are for getting the optimal cutting force is at a cutting speed of 20 m/min, feed rate of 0.26 mm/rev, and a depth of cut of 0.3 mm.
- ii) Surface finish was improved when the turning was performed at a cutting speed of 17 m/min, feed rate 0.26 mm/rev, and depth of cut 0.3 mm.
- iii) In order to remove the maximum amount of material, a cutting speed of 17 m/min, a feed rate of 0.33 mm/rev, and a cut depth of 0.1 mm is required.
- iv) For experiencing a reduced temperature during the turning process, a cutting force of 14 m/min, feed rate of 0.26 mm/rev, and depth of cut of 0.3 mm is selected.
- v) The Feed rate was found to be the most significant process parameter for getting higher cutting force and material removal rate. The Cutting speed was found to be the most influencing process for getting lower surface roughness and temperature.
- vi) The optimal parameter combination obtained from Taguchi GRA for getting better output response was at a cutting speed of 14 m/min, feed rate of 0.33 mm/rev, depth of cut at 0.3 mm.
- vii) From ANOVA Feed rate has the maximum contribution of 77.38% followed by cutting speed having 8.65% and a minimum contribution by Depth of cut having 0.41%.

9. BIBLIOGRAPHY

- [1] LEARY, M., MAZUR, M., WILLIAMS, H., *et al.*, "Inconel 625 lattice structures manufactured by selective laser melting (SLM): mechanical properties, deformation and failure modes", *Materials & Design*, v. 157, pp. 179–199, 2018. doi: <http://doi.org/10.1016/j.matdes.2018.06.010>.
- [2] GONZALEZ, J.A., MIRELES, J., STAFFORD, S.W., *et al.*, "Characterization of Inconel 625 fabricated using powder-bed-based additive manufacturing technologies", *Journal of Materials Processing Technology*, v. 264, pp. 200–210, 2019. doi: <http://doi.org/10.1016/j.jmatprotec.2018.08.031>.
- [3] WAGHMODE, S.P., DABADE, U.A., "Optimization of process parameters during turning of Inconel 625", *Materials Today: Proceedings*, v. 19, pp. 823–826, 2019. doi: <http://doi.org/10.1016/j.matpr.2019.08.138>.

- [4] AKGÜN, M., DEMIR, H., “Optimization of cutting parameters affecting surface roughness in turning of inconel 625 superalloy by cryogenically treated tungsten carbide inserts”, *SN Applied Sciences*, v. 3, n. 2, pp. 277, 2021. doi: <http://doi.org/10.1007/s42452-021-04303-2>.
- [5] REDDY, M., WILLIAM, L., “Finite Element analysis: predicting cutting force in turning of Inconel 625 using ceramic tools”, *IOP Conference Series. Materials Science and Engineering*, v. 943, n. 1, pp. 012019, 2020. doi: <http://doi.org/10.1088/1757-899X/943/1/012019>.
- [6] BADEMLIOGLU, A.H., CANBOLAT, A.S., YAMANKARADENIZ, N., *et al.*, “Investigation of parameters affecting Organic Rankine Cycle efficiency by using Taguchi and ANOVA methods”, *Applied Thermal Engineering*, v. 45, pp. 221–228, 2018. doi: <http://doi.org/10.1016/j.applthermaleng.2018.09.032>.
- [7] BHARDWAJ, T., SHUKLA, M., PAUL, C.P., *et al.*, “Direct energy deposition-laser additive manufacturing of titanium-molybdenum alloy: parametric studies, microstructure and mechanical properties”, *Journal of Alloys and Compounds*, v. 787, pp. 1238–1248, 2019. doi: <http://doi.org/10.1016/j.jallcom.2019.02.121>.
- [8] BIN, L.I.U., BAO-QIANG, L.I., ZHONGHUA, L.I., *et al.*, “Selective laser remelting of an additive layer manufacturing process on AlSi10Mg”, *Results in Physics*, v. 12, pp. 982–988, 2019. doi: <http://doi.org/10.1016/j.rinp.2018.12.018>.
- [9] RAKESH, P.R., CHAKRADHAR, D., “Machining performance comparison of Inconel 625 superalloy under sustainable machining environments”, *Journal of Manufacturing Processes*, v. 85, pp. 742–755, 2023. doi: <http://doi.org/10.1016/j.jmapro.2022.11.080>.
- [10] RIVERA, O.G., ALLISON, P.G., JORDON, J.B., *et al.*, “Microstructures and mechanical behavior of inconel 625 fabricated by solid-state additive manufacturing”, *Materials Science and Engineering A*, v. 694, pp. 1–9, 2017. doi: <http://doi.org/10.1016/j.msea.2017.03.105>.
- [11] LI, C., WHITE, R., FANG, X.Y., *et al.*, “Microstructure evolution characteristics of inconel 625 alloy from selective laser melting to heat treatment”, *Materials Science and Engineering A*, v. 705, pp. 20–31, 2017. doi: <http://doi.org/10.1016/j.msea.2017.08.058>.
- [12] LIU, E., AN, W., XU, Z., *et al.*, “Experimental study of cutting-parameter and tool life reliability optimization in inconel 625 machining based on wear map approach”, *Journal of Manufacturing Processes*, v. 53, pp. 34–42, 2020. doi: <http://doi.org/10.1016/j.jmapro.2020.02.006>.
- [13] VENKATESAN, K., RAMANUJAM, R., *et al.*, “Influence of cutting parameters on dry machining of inconel 625 alloy with coated carbide insert - a statistical approach”, *Journal of Engineering and Applied Sciences (Asian Research Publishing Network)*, v. 9, pp. 250–258, 2014.
- [14] RAJGURU, R.R., VASUDEVAN, H., “A study of micro hardness in the machining of inconel 625 using TiAlSiN coated tools under dry cutting conditions”, *Advances in Materials and Processing Technologies*, v. 10, pp. 120–130, 2024. doi: <http://doi.org/10.1080/2374068X.2022.2100035>.
- [15] KREBS, G., POLLI, M.L., “Cutting parameters for roughing turning of alloy 625 clad using ceramic inserts”, *Materials Research*, v. 22, n. 1, pp. e20190535, 2019. doi: <http://doi.org/10.1590/1980-5373-mr-2019-0535>.
- [16] RAKESH, P.R., CHAKRADHAR, D., “Multi-response optimisation and performance evaluation of Inconel 625 superalloy machining under cryogenic cooling environment”, *Advances in Materials and Processing Technologies*, v. 10, n. 3, pp. 1303–1319, 2023. doi: <http://doi.org/10.1080/2374068X.2023.2189612>.
- [17] SINGH, T., DUREJA, J.S., DOGRA, M., *et al.*, “Environment friendly machining of Inconel 625 under nano-fluid minimum quantity lubrication (NMQL)”, *International Journal of Precision Engineering and Manufacturing*, v. 19, n. 11, pp. 1689–1697, 2018. doi: <http://doi.org/10.1007/s12541-018-0196-7>.
- [18] ÖZBEK, N.A., ÖZBEK, O., KARA, F., “Statistical analysis of the effect of the cutting tool coating type on sustainable machining parameters”, *Journal of Materials Engineering and Performance*, v. 30, n. 10, pp. 7783–7795, 2021. doi: <http://doi.org/10.1007/s11665-021-06066-8>.
- [19] AKGÜN, M., KARA, F., “Analysis and optimization of cutting tool coating effects on surface roughness and cutting forces on turning of AA 6061 alloy”, *Advances in Materials Science and Engineering*, v. 2021, n. 1, pp. 6498261, 2021. doi: <http://doi.org/10.1155/2021/6498261>.
- [20] BATISTA, V.R., PEREIRA, E.M.A., FRAGA, R.D.C.F., *et al.*, “Effect of stress relief heat treatment and preheating on the microstructure and microhardness of the interface between Inconel 625 deposit and AISI 8630M and AISI 4130 steels”, *Matéria (Rio de Janeiro)*, v. 26, pp. e12920, 2021. doi: <http://doi.org/10.1590/s1517-707620210001.1220>.

- [21] YANG, T., LIU, T., LIAO, W., *et al.*, “The influence of process parameters on vertical surface roughness of the AlSi10Mg parts fabricated by selective laser melting”, *Journal of Materials Processing Technology*, v. 266, pp. 26–36, 2019. doi: <http://doi.org/10.1016/j.jmatprotec.2018.10.015>.
- [22] LIU, E., AN, W., XU, Z., *et al.*, “Experimental study of cutting-parameter and tool life reliability optimization in inconel 625 machining based on wear map approach”, *Journal of Manufacturing Processes*, v. 53, pp. 34–42, 2020. doi: <http://doi.org/10.1016/j.jmapro.2020.02.006>.
- [23] VISAGAN, A., GANESH, P., “A hybrid optimization approach of single point incremental sheet forming of aisi 316l stainless steel using grey relation analysis coupled with principal component analysis”, *Journal of Wuhan University of Technology-Mater*, v. 39, n. 1, pp. 160–166, 2024. doi: <http://doi.org/10.1007/s11595-024-2867-9>.
- [24] VISAGAN, A., GANESH, P., “Parametric optimization of two point incremental forming using GRA and TOPSIS”, *International Journal of Simulation Modelling*, v. 21, n. 4, pp. 615–626, 2022. doi: <http://doi.org/10.2507/IJSIMM21-4-622>.
- [25] VISAGAN, A., GANESH, P., ETHIRAJ, N., *et al.*, “Multi objective optimization of single point incremental forming of 316L stainless steel using grey relational and principal component analyses”, *Transactions of FAMENA*, v. 48, n. 2, pp. 85–89, 2024. doi: <http://doi.org/10.21278/TOF.482054923>.
- [26] VENKATESAN, K., NAGENDRA, K.U., ANUDEEP, C.M., *et al.*, “Experimental investigation and parametric optimization on hole quality assessment during micro-drilling of Inconel 625 Super alloy”, *Arabian Journal for Science and Engineering*, v. 46, n. 3, pp. 2283–2309, 2021. doi: <http://doi.org/10.1007/s13369-020-04992-8>.